Chapter 8

Observational Constraints on MCG in Horava-Lifshitz Gravity with Dark Radiation

8.1 Introduction

In the previous Chapter cosmological models in HL gravity is studied in the presence of detailed balance condition and projectibility. Sotiriou, Visser and Weinfurtner (SVW) [225, 226] proposed another form of HL gravity with projectibility assuming beyond detailed balance condition which will be considered here. In a spatially curved Friedmann-Robertson-Walker universe, the SVW generalization yields an extra $\frac{1}{a^6}$ - term in the field equation compared to detailed balance scenario. Under this condition the field equations are modified in which a term similar to radiation known as dark radiation is found to exist. The EoS parameters of MCG in beyond detailed balance

scenario in presence of dark radiation is constrained here using observational data.

8.2 HL cosmology with beyond detailed balance condition and projectibility

As the scope of information with detailed balance condition is not enough for understanding observed universe in HL gravity [82, 83], in this section we investigate cosmologies in the HL gravity relaxing the detailed balance condition. Considering modified Chaplygin gas (MCG), baryon, radiation and dark radiation without detailed balance in the framework of HL gravity cosmological models are obtained. The motivation of considering such model is to explore the effects of the dark radiation on the parameters of the MCG model employing observational data. The Friedmann equations in this case can be written as [225, 226, 227, 235, 236, 237]:

$$\begin{aligned} H^2 &= \frac{2\sigma_0}{(3\lambda-1)}(\rho_m+\rho_r) \\ &\quad +\frac{2}{(3\lambda-1)}\left[\frac{\sigma_1}{6}+\frac{\sigma_3 K^2}{6a^4}+\frac{\sigma_4 K}{6a^6}\right]+\frac{\sigma_2 K}{3(3\lambda-1)a^2}, \end{aligned} \tag{8.1}$$

$$\begin{aligned} \dot{H}+\frac{3}{2}H^2 &= \frac{3\sigma_0}{(3\lambda-1)}(\rho_m\omega_m+\rho_r\omega_r) \\ &\quad -\frac{3}{(3\lambda-1)}\left[-\frac{\sigma_1}{6}+\frac{\sigma_3 K^2}{18a^4}+\frac{\sigma_4 K}{6a^6}\right]+\frac{\sigma_2 K}{6(3\lambda-1)a^2}, \end{aligned} \tag{8.2}$$

where $\sigma_0 = \kappa^2/12$, we define some useful dimensionless parameters, given below

$$G_{cosmo}=\frac{6\sigma_0}{8\pi(3\lambda-1)}, \sigma_2=-3(3\lambda-1), G_{grav}=\frac{6\sigma_0}{16\pi}, \tag{8.3}$$

where $\sigma_2 < 0$ and $\sigma_4 > 0$. In the case of the beyond detailed balance condition and in the IR limit ($\lambda = 1$), the two parameters G_{cosmo} and G_{grav} become equal.

8.3 Observational constraints on EoS parameters

The EoS parameters of MCG given by eq. (1.3) are to be determined here for viable cosmologies in the framework of HL gravity using the recent observational data namely, Observed Hubble data (OHD), BAO peak parameter and CMB shift parameter.

8.3.1 Constraints obtained from beyond detailed balance

In beyond detailed balance scenario for $\lambda = 1$, the field eqs. (8.1) and (8.2) become

$$H^2 = \frac{8\pi G}{3}(\rho_b + \rho_c + \rho_r) + \left[\frac{\sigma_1}{6} + \frac{\sigma_3 K^2}{6a^4} + \frac{\sigma_4 K}{6a^6}\right] - \frac{K}{a^2} \tag{8.4}$$

$$\dot{H} + \frac{3}{2}H^2 = -4\pi G(p_c + \frac{1}{3}\rho_r) - \frac{3}{2}\left[-\frac{\sigma_1}{6} + \frac{\sigma_3 K^2}{18a^4} + \frac{\sigma_4 K}{6a^6}\right] - \frac{K}{2a^2}. \tag{8.5}$$

Finally, a dimensionless Hubble parameter ($E(z)$) can be obtained as

$$\begin{aligned} E^2(z) &= \Omega_{b0}(1+z)^3 + \Omega_{c0}F(z) + \Omega_{r0}(1+z)^4 + \Omega_{K0}(1+z)^2 \\ &\quad + [\Omega_1 + \Omega_3(1+z)^4 + \Omega_4(1+z)^6] \end{aligned} \tag{8.6}$$

where $F(z) = \left[A_s + \frac{1-A_s}{a^{3(1+B)(1+\alpha)}}\right]^{\frac{1}{1+\alpha}}$. The dimensionless parameters, namely, Ω_1, Ω_3, Ω_4 are related to the model parameters σ_1, σ_3, σ_4 as follows:

$$\Omega_1 = \frac{\sigma_1}{6H_0^2},\ \Omega_3 = \frac{\sigma_3 H_0^2 \Omega_{K0}^2}{6},\ \Omega_4 = -\frac{\sigma_4 \Omega_{K0}}{6}. \tag{8.7}$$

At the present epoch $E(z=0) = 1$, it leads to

$$\Omega_{b0} + \Omega_{c0} + \Omega_{r0} + \Omega_{K0} + \Omega_1 + \Omega_3 + \Omega_4 = 1. \tag{8.8}$$

In the above equations Ω_4 is required to be a positive quantity in order that the Hubble parameter and the gravitational perturbations [225, 226, 235] are positive definite at all values of redshifts. Ω_3 is also assumed to be positive definite. Following the procedure adopted in Ref. [218] for ΔN_ν, we consider the upper limit of dark radiation in the standard model from the Big Bang Nucleo-synthesis (BBN). Consequently, at the time of BBN ($z = z_{BBN}$) [228, 229, 230, 238] we get :

$$\Omega_3 + \Omega_4(1 + z_{BBN}^2)^2 = \Omega_{3max} = 0.135\Delta N_\nu \Omega_{r0}, \tag{8.9}$$

where the Ω_3 represents the usual dark radiation and Ω_4 represents a kinetic-like component (a quintessence field dominated by kinetic energy) [239, 240]. The above equation will be used to replace Ω_4 in terms of other parameters in the analysis. For simplicity we define

$$\beta = \frac{\Omega_3}{\Omega_{3max}} \tag{8.10}$$

where Ω_{3max} is the upper limit on Ω_3. Consequently Ω_3 can be expressed in terms of the other parameters. Following the detailed balance scenario we consider ΔN_ν, so that it satisfies the bound $0 < \Delta N_\nu \leq 2.0$, taking into account the importance of curvature in dark energy models and treating Ω_{K0} as a free parameter as was taken in Ref. ([241, 242]). The Hubble parameter contains thirteen free parameters, namely, Ω_{b0}, Ω_{c0}, Ω_{r0}, Ω_{K0}, Ω_1, Ω_3, Ω_4, ΔN_ν, H_0, A_s, B, α, β. To analyze numerically some of them are fixed using the best-fit values from WMAP 7 data [93]. The parameters are $\Omega_{m0}(\equiv \Omega_{b0} + \Omega_{c0})$, Ω_{b0}, H_0, Ω_{r0} and the corresponding values of the parameters are chosen as follows: $\Omega_{m0} = 0.27$, $\Omega_{b0} = 0.04$, $H_0 = 71.4 Km/sec/Mpc$, $\Omega_{r0} = 8.14 \times 10^{-5}$. Using the constraint eqs. (8.7) - (8.10) one can replace Ω_1, Ω_3, Ω_4 in terms of the other six free parameters for the numerical analysis. Thus six free

parameters are left to be determined which are Ω_{K0}, A_s, B, α, β, ΔN_ν.

To determine the constraints on the parameters of the MCG in beyond detailed balance scenario, we consider three values of α satisfying $0 \leq \alpha \leq 1$ (α=0.999, 0.500, 0.001) and determine the best-fit values for the rest five parameters (*i.e.*, A_s, B, β, Ω_{K0}, ΔN_ν). Thereafter, at the best-fit value of ΔN_ν, β, Ω_{K0} for three values of α we plot 2d contours for the pair of parameters (A_s, B) at different confidence levels. The contours of A_s, B drawn at different values of α, determines the permissible range of values of the B parameter for the MCG in HL gravity in the framework of beyond detailed balance scenario. The effect of dark radiation (*i.e.*, effective neutrino parameter) on the constraints on the parameters of the MCG, is studied here considering two extreme values of α (α=0.999, 0.001) in the limit $0 \leq \alpha \leq 1$ for the two extreme values of ΔN_ν (0.01, 2.0). In this case each of these values of α , ΔN_ν determines the best-fit values of the rest four parameters (*i.e.*, A_s, B, β, Ω_{K0}). Thereafter, at the extreme values of ΔN_ν for two extreme values of α we plot 2d contours for the parameters A_s, B for the best-fitted values of β, Ω_{K0} at different confidence levels. From the contours of A_s, B drawn at different values of α and ΔN_ν we determine the permissible range of values of the B parameter for the MCG in HL gravity in the framework of beyond detailed balance scenario. We note that the range of values of B is narrower due to the effect of effective neutrino parameter on B.

8.4 Numerical analysis

In this section, we determine constraints on the parameters of the MCG in beyond detailed balance scenario employing observed data namely, Stern data set for $(H(z)-$

z) data (OHD), BAO peak parameter and CMB shift parameter. We adopt numerical technique to determine the constraints with the help of a *Chi-square* function. The limiting values for the EoS parameters are determined by minimization the *Chi-square* function thereafter.

8.4.1 (H-z) data (OHD) as a tool for constraining

The *Chi-square* function is defined as

$$\chi^2_{OHD}(H_0, \Omega_{K0}, A_s, B, \alpha, \beta, \Delta N_\nu, z) = \sum \frac{(H(H_0, \Omega_{K0}, A_s, B, \alpha, \beta, \Delta N_\nu, z) - H_{obs}(z))^2}{\sigma_z^2} \tag{8.11}$$

where $H_{obs}(z)$ is the observed Hubble parameter at redshift z and σ_z is the associated error with that particular observation. Hubble parameter is given by

$$H(z) = H_0 E(z) \tag{8.12}$$

where

$$\begin{aligned} E^2(z) &= \Omega_{b0}(1+z)^3 + \Omega_{c0}F(z) + \Omega_{r0}(1+z)^4 + \Omega_{K0}(1+z)^2 \\ &\quad + [\Omega_1 + \Omega_3(1+z)^4 + \Omega_4(1+z)^6] \end{aligned} \tag{8.13}$$

with $F(z) = \left[A_s + \frac{1-A_s}{a^{3(1+B)(1+\alpha)}}\right]^{\frac{1}{1+\alpha}}$. Here $(H(z) - z)$ data (OHD) is taken from Stern data analysis [99] which is shown in Table-(2.1).

8.4.2 BAO peak parameter as a tool for constraining

The *Chi-square* function χ^2_{BAO} given by eq. (1.31) with $\mathcal{A}$ $(0.469 \pm .0.017)$ from the SDSS (Sloan Digital Sky Survey) data for LRG (Luminous Red Galaxies) survey [88] is used here for numerical analysis.

Data	CL	B
$\alpha = 0.999$	68.3%	$(-0.0550,\ 0.0381)$
	95.4%	$(-0.0799,\ 0.0735)$
	99.7%	$(-0.1035,\ 0.1128)$
$\alpha = 0.500$	68.3%	$(-0.0574,\ 0.0442)$
	95.4%	$(-0.0835,\ 0.0829)$
	99.7%	$(-0.1060,\ 0.1305)$
$\alpha = 0.001$	68.3%	$(-0.0926,\ 0.0707)$
	95.4%	$(-0.1326,\ 0.1493)$
	99.7%	$(-0.1727,\ 0.2247)$

Table 8.1: Range of values of the EoS parameters in beyond detailed balance scenario

8.4.3 CMB shift parameter as a tool for constraining

The definition of CMB shift parameter given by eq. (1.34) with the WMAP 7 data giving $R = 1.726 \pm 0.018$ at $z = 1091.3$ [93] is also used to define a *Chi-square* function χ^2_{CMB}.

8.4.4 Joint analysis with OHD + BAO+ CMB data

The total *Chi-square* function for the joint analysis is given by:

$$\chi^2_{tot} = \chi^2_{OHD} + \chi^2_{BAO} + \chi^2_{CMB}. \tag{8.14}$$

The statistical analysis with χ^2_{tot} gives the bounds on the model parameter specially on B. Range of values of the EoS parameters in beyond detailed balance scenario are shown in Table-(8.1). Fig. (8.1 a) is plotted for $\alpha = 0.999$ with best-fitted values of β, ΔN_ν and Ω_{K0}. The parameter B lies in $(-0.0550,\ 0.0381)$, $(-0.0799,\ 0.0735)$, $(-0.1035,\ 0.1128)$ at 68.3%, 95.4%, 99.7% confidence levels respectively. Fig. (8.1 b) is plotted for $\alpha = 0.500$ for best-fitted values of β, ΔN_ν and Ω_{K0}. The parameter B in this case satisfies the following limits: $(-0.0574,\ 0.0442)$,

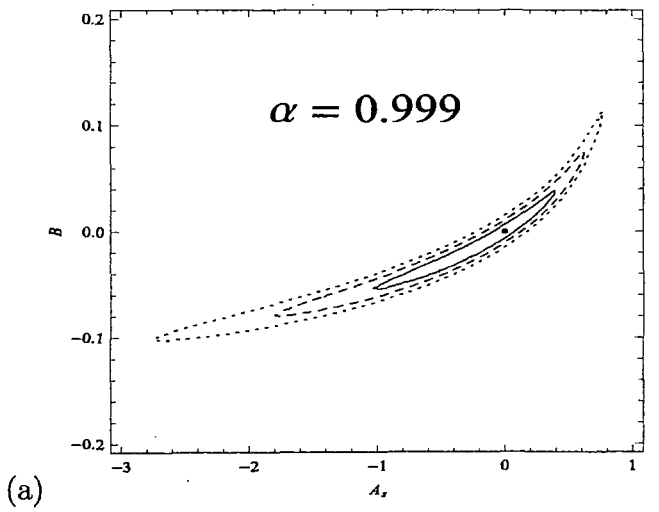

(a)

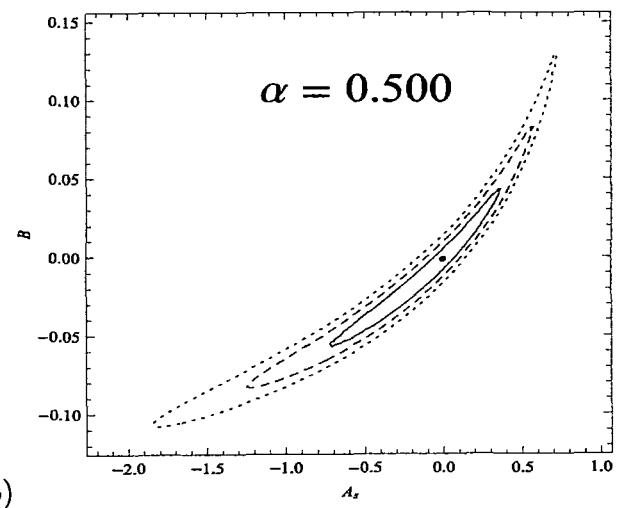

(b)

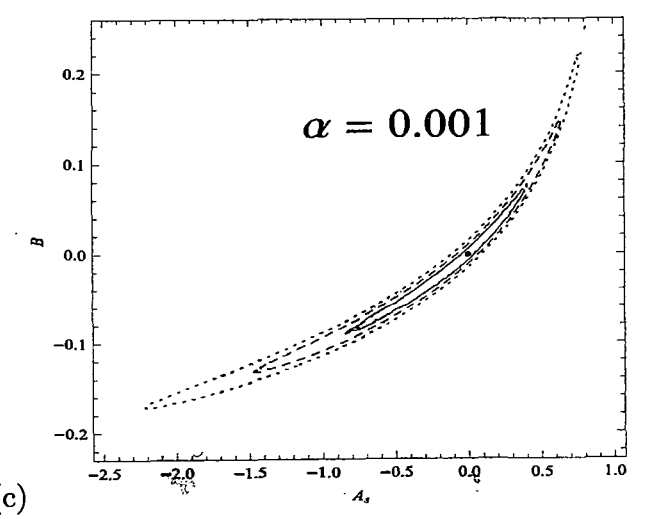

(c)

Figure 8.1: $A_s - B$ contours for (a) $\alpha = 0.999$, (b) $\alpha = 0.500$ and (c) $\alpha = 0.001$ in beyond detailed balance scenario using ($OHD + SDSS\ (BAO) + CMB$ shift) data at 68.3% (Solid), 95.4% (Dashed) and 99.7% (Dotted) confidence level.

Data	*CL*	*B*
$\alpha = 0.999, \Delta N_\nu = 0.01$	68.3%	(−0.0534, 0.0335)
	95.4%	(−0.0794, 0.0745)
	99.7%	(−0.1013, 0.1224)
$\alpha = 0.999, \Delta N_\nu = 2.0$	68.3%	(−0.0546, 0.0362)
	95.4%	(−0.0798, 0.0766)
	99.7%	(−0.1032, 0.1162)

Table 8.2: Acceptable range of B parameter in beyond detailed balance scenario for $\alpha = 0.999$

(−0.0835, 0.0829), (−0.1060, 0.1305) at 68.3%, 95.4%, 99.7% confidence levels respectively. Fig. (8.1 c) is plotted for $\alpha = 0.001$ for best-fitted value of β, ΔN_ν and Ω_{K0}. We note that the parameter B satisfies the following limiting values (−0.0926, 0.0707), (−0.1326, 0.1493), (−0.1727, 0.2247) at 68.3%, 95.4%, 99.7% confidence levels respectively. It is evident that the allowed range of values of the parameter B is wider compared to that of the detailed balance scenario [243]. The range of B parameter in beyond detailed balance scenario for one extreme alpha ($\alpha = 0.999$) is shown in Table-(8.2). Fig. (8.2 a) is plotted for $\alpha = 0.999$ and ΔN_ν=0.01 with best-fitted value of β and Ω_{K0}. It is evident that B can take both positive and negative values in the ranges: (−0.0534, 0.0335), (−0.0794, 0.0745), (−0.1013, 0.1224) at 68.3%, 95.4%, 99.7% confidence levels respectively. Fig. (8.2 b) is plotted for $\alpha = 0.999$ and ΔN_ν=2.0, it is evident that the value of B lies in the range (−0.0546, 0.0362), (−0.0798, 0.0766), (−0.1032, 0.1162) at 68.3%, 95.4%, 99.7% confidence levels respectively. The figs. (8.2 a - 8.2 b) show that the range of permissible values of B decreases with an increase in the effective neutrino parameter. The range of B parameter in beyond detailed balance scenario for smaller alpha ($\alpha = 0.001$) are shown in Table-(8.3) at different confidence limit. Fig. (8.3

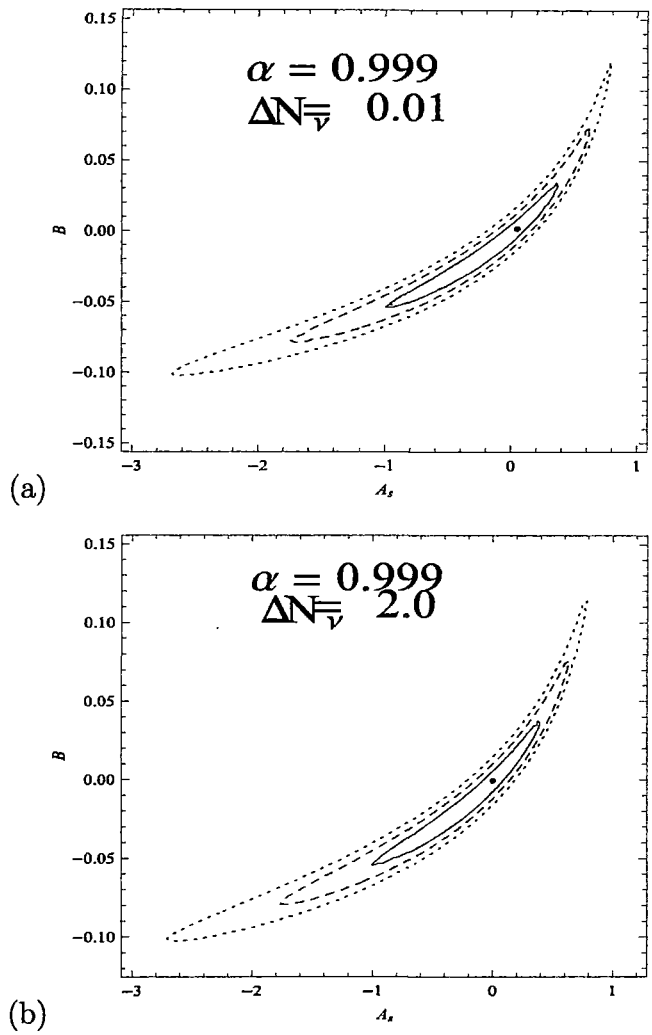

Figure 8.2: Constraints in beyond detailed balance for $\alpha = 0.999$ using ($OHD + SDSS\ (BAO) + CMB$ shift) data at 68.3% (Solid), 95.4% (Dashed) and 99.7% (Dotted) confidence level.

Data	*CL*	*B*
$\alpha = 0.001, \Delta N_\nu = 0.01$	68.3%	(−0.0668, 0.0407)
	95.4%	(−0.0943, 0.0892)
	99.7%	(−0.1206, 0.1416)
$\alpha = 0.001, \Delta N_\nu = 2.0$	68.3%	(−0.0635, 0.0484)
	95.4%	(−0.0924, 0.0924)
	99.7%	(−0.1194, 0.1414)

Table 8.3: Acceptable range of B parameter in beyond detailed balance scenario for $\alpha = 0.001$

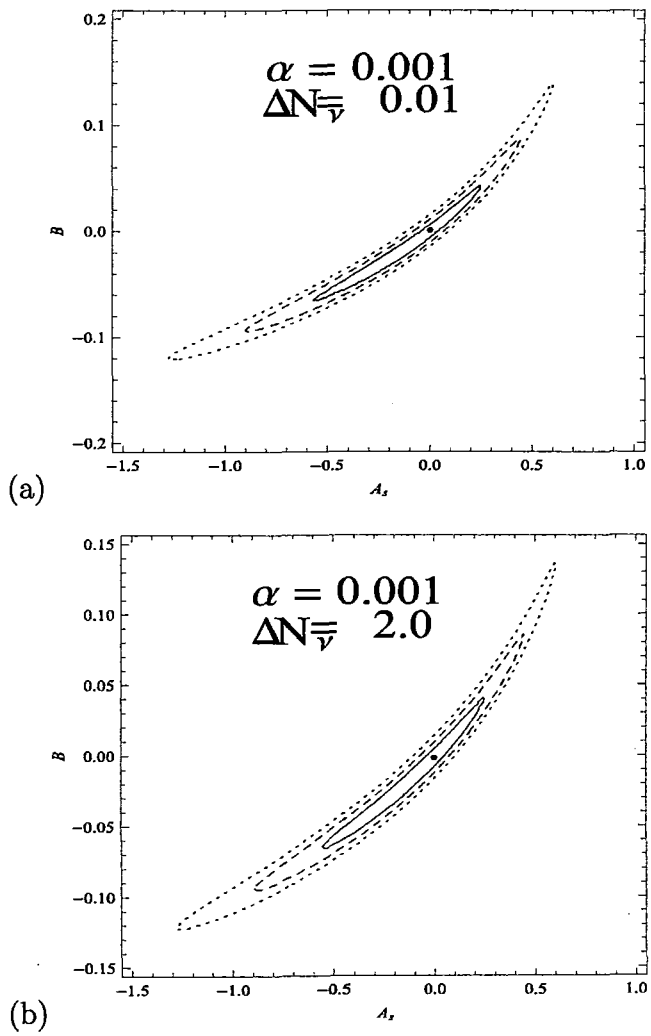

Figure 8.3: Constraints in beyond detailed balance for $\alpha = 0.001$ using ($OHD + SDSS\ (BAO) + CMB$ shift) data at 68.3% (Solid), 95.4% (Dashed) and 99.7% (Dotted) confidence level.

a) is plotted for $\alpha = 0.001$ and ΔN_ν=0.01 for best-fitted value of β and Ω_{K0}, it is evident that the permissible values of B now lies in the range $(-0.0668,\ 0.0407)$, $(-0.0943,\ 0.0892)$, $(-0.1206,\ 0.1416)$ at 68.3%, 95.4%, 99.7% confidence levels respectively. Fig. (8.3 b) is plotted for $\alpha = 0.001$ and ΔN_ν=2.0, it is evident that the values of B lies in the range $(-0.0635,\ 0.0484)$, $(-0.0924,\ 0.0924)$, $(-0.1194,\ 0.1414)$ at 68.3%, 95.4%, 99.7% confidence levels respectively. The contours drawn in figs. (8.3 a) and (8.3 b) show that the range of permissible values of B now decreases with an increase in the effective neutrino parameter. It is noted that the allowed range of values of the parameter B, decreases appreciably here compared to that permitted from figs. (8.1 a - 8.1 c). This signifies the fact that as the contribution of dark radiation increases (through effective neutrino parameter) the range of admissible values of B decreases in the case of beyond detailed balance scenario.

8.5 Viability of MCG in HL gravity

In the case of beyond detailed balance scenario the total pressure and the energy density is given respectively as

$$p_{tot} = p_c + \frac{1}{3}\rho_r + \left[-\frac{\sigma_1}{6\sigma_0} + \frac{\sigma_3 K^2}{18\sigma_0 a^4} + \frac{\sigma_4 K}{6\sigma_0 a^6}\right], \tag{8.15}$$

$$\rho_{tot} = \rho_c + \rho_b + \rho_r + \left[\frac{\sigma_1}{6\sigma_0} + \frac{\sigma_3 K^2}{6\sigma_0 a^4} + \frac{\sigma_4 K}{6\sigma_0 a^6}\right]. \tag{8.16}$$

In the above equations the scale factor is replaced by redshift parameter and consequently the density parameter and the Hubble parameter can be expressed in terms of redshift parameter. The EoS parameter in terms of the redshift parameter z is

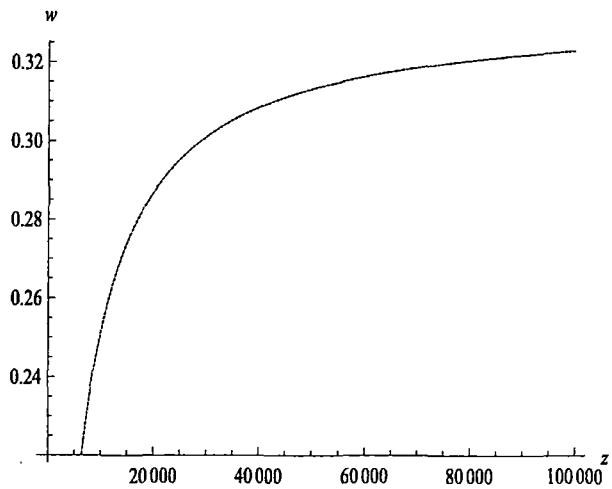

Figure 8.4: Equation of state parameter in beyond detailed balance scenario

given by

$$w(z) = \frac{p_{tot}}{\rho_{tot}}. \tag{8.17}$$

From the plot of $w(z)$ with z, for beyond detailed balance scenario we note that at high redshift (*i.e.*, early times) it attains a fixed value $\frac{1}{3}$ since radiation dominates in that epoch. In the intermediate redshift it behaves as dust for quite a long time. It is observed that the equation of state parameter picks up negative values at small redshift, *i.e.*, in the recent past. The present value of the equation of state parameter attains a negative value (-0.7) in the case of closed or open universe. In order to test the validity of cosmological models, the best-fit values of the parameters of MCG are employed for drawing curve for supernovae magnitudes (μ) at different redshift (z). We also plot μ *vs.* z curve to compare with observation. The plot of Union2 data [244] from the observations is in excellent agreement with the model.

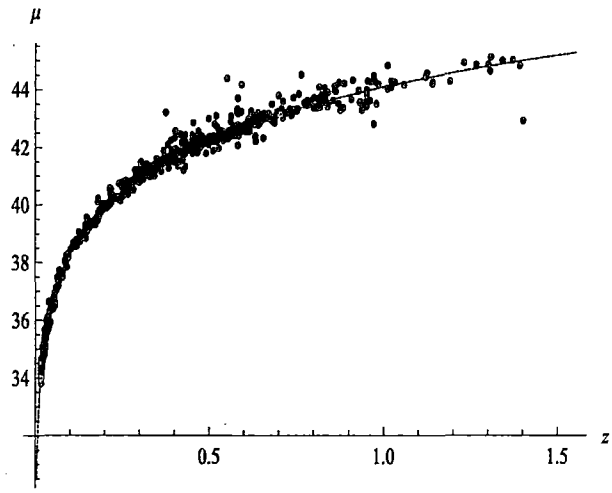

Figure 8.5: The comparison of the Union2 data with the best-fit values in beyond detailed balance

8.6 Discussion

Cosmological models with MCG in HL gravity scenario are studied considering beyond detailed balance conditions both in the presence and in the absence of dark radiation. Constraints on EoS parameters are determined using observational data namely, $(H(z) - z)$ (OHD), BAO peak parameter, CMB shift parameter data. For the MCG, the parameter B corresponds to the matter part. The allowed range of values of B for viable cosmologies are determined.

In the beyond detailed balance scenario there are six free parameters, namely Ω_{K0} , A_s, B, α, β, ΔN_ν. It is found that the entire range of effective neutrino parameter is consistent with observations from our numerical analysis. The contours drawn in figs. (8.1 a - 8.1 c) for beyond detailed balance condition with whole range of α for best-fitted values of other parameters (β, ΔN_ν and Ω_{K0}) projects the admissible values of B that lies in the range $(-0.0926, 0.0707)$, $(-0.1326, 0.1493)$, $(-0.1727, 0.2247)$

(Table-8.1) at 68.3%, 95.4%, 99.7% confidence levels respectively. The range of B obtained for beyond detailed balance scenario are found larger than that of detailed balance scenario and without dark radiation [243]. It is evident from figs. (8.2 a - 8.2 b) that the permitted range of values of B decreases with an increase of the effective neutrino parameter for $\alpha = 0.999$. It is also evident from fig. (8.3) for $\alpha = 0.001$ with different (ΔN_ν) that the range of values of B decreases with an increase of the effective neutrino parameter. It is noted that the range of values of B decreases appreciably here compared to that obtained from figs. (8.1 a - 8.1 c). This signifies that as the contribution of dark radiation increases (through effective neutrino parameter) the contribution in the permissible range of values of B decreases in beyond detailed balance scenario. In figure (8.4) we plot the variation of the equation of state parameter $w(z)$ with the redshift parameter z for beyond detailed balance scenario. The curve shows the evolutionary phases of the universe satisfactorily. It is evident that at high redshift (early times) the equation of state parameter attains $\frac{1}{3}$, indicating radiation domination phase in that epoch. However, in the intermediate redshift we note that dust dominates and MCG dominates in recent times for quite a long period. Using the best-fit values in beyond detailed balance scenario we plot μ *vs.* redshift curve in fig. (8.5) and the figure is then compared with the Union Compilation data [244]. It is evident from the figure that cosmologies in HL gravity with MCG fits well with the experimental result.